Chip-Based Optical Isolator and Nonreciprocal Parity-Time Symmetry Induced by Stimulated Brillouin Scattering

Jiyang Ma, Jianming Wen, Shulin Ding, Shengjun Li, Yong Hu, Xiaoshun Jiang,* Liang Jiang, and Min Xiao

Realization of chip-scale nonreciprocal optics such as isolators and circulators is highly demanding for all-optical signal routing and protection with standard photonics foundry process. Owing to the significant challenge for incorporating magneto-optical materials on chip, the exploration of magnetic-free alternatives has become exceedingly imperative in integrated photonics. Here, a chip-based, tunable all-optical isolator at the telecommunication band is demonstrated, which is based upon bulk stimulated Brillouin scattering (SBS) in a high-Q silica microtoroid resonator. This device exhibits remarkable characteristics over most state-of-the-art implements, including high isolation ratio, no insertion loss, and large working power range. Thanks to the guided acoustic wave and accompanying momentum-conservation condition, bulk SBS also assist in realizing the nonreciprocal parity-time symmetry in two directly coupled microresonators. The breach of time-reversal symmetry further makes the design a versatile arena for developing many formidable ultra-compact devices such as unidirectional single-mode Brillouin lasers and supersensitive photonic sensors.

1. Introduction

Integrated photonic circuits demand dynamic optical isolation for advanced signal processing and communications. For the

Dr. J. Ma, Dr. S. Ding, S. Li, Y. Hu, Prof. X. Jiang, Prof. M. Xiao
National Laboratory of Solid State Microstructures, College of Engineering and Applied Sciences, and School of Physics
Nanjing University
Nanjing 210093, China
E-mail: jxs@nju.edu.cn

Prof. J. Wen
Department of Physics
Kennesaw State University
Marietta, GA 30060, USA

Prof. L. Jiang
Pritzker School of Molecular Engineering
University of Chicago
Chicago, IL 60637, USA

Prof. M. Xiao
Department of Physics
University of Arkansas
Fayetteville, AR 72701, USA

time-reversal symmetry retained in light–matter interaction, unfortunately, light wave transport in any linear, time-invariant optical system complies with the Lorentz reciprocity.[1,2] To violate such reciprocity and obtain asymmetric transmission, it essentially requires to break the time-reversal symmetry. In optics this is typically achievable by employing the magneto-optic Faraday effect. Despite its commercial success, such a well-established approach poses a severe challenge[3,4] for the incorporation with chip-scale photonics due to fabrication complexity with the mature complementary metal–oxide semiconductor (CMOS) technique and difficulty in locally confining magnetic fields as well as significant material losses. As a result, a vibrant search for different physical principles to obtain magnetic-free optical nonreciprocity has garnered a vast impetus in recent years. Alternative methods mostly resort to indirect interband transitions,[5–7] nonlinear parametric amplification,[8,9] thermo-optic effect,[10] opto-acoustic interaction,[11] Raman amplification,[12] stimulated Brillouin scattering (SBS),[13,14] Bragg scattering,[15] gain/absorption saturation,[16] Kerr nonlinearities,[17,18] optomechanical interactions,[19–26] and mimicked nonlinear nonadiabatic quantum jumps.[27] Of these schemes, asymmetric optical transmission is mostly experimented with only injecting a light wave in either forward or backward direction. The drawbacks in this type of implementation were questioned in a theoretical study,[28] where they showed simultaneous presence of signals from both sides incapable of providing complete isolation for Kerr or Kerr-type nonlinearities, due to dynamic reciprocity. Although chip-based optical isolators based on the magneto-optic Faraday effect,[3,4,29] interband photonic transition[5–7] and optomechanical effect[19–26] as well as the optical nonlinearity[8,18] are not bounded by this limitation in principle, only few works[8,18,25] experimentally demonstrated the true chip-based optical isolators, by injecting signal waves from both sides simultaneously.

In parallel to the rapid progress on on-chip optical nonreciprocity, there has been an intense research interest in non-Hermitian photonic systems.[30,31] This originates from the observation[32] that certain non-Hermitian Hamiltonians retaining the combined parity-time (PT) symmetry may have real

**ADVANCED
SCIENCE NEWS**

www.advancedsciencenews.com

LASER
& PHOTONICS
REVIEWS

www.lpr-journal.org

spectra as long as a non-Hermitian parameter reaches above a specific threshold value. At threshold, PT symmetry breaking spontaneously occurs, where the system transitions to a new phase associated with a pair of complex eigenvalues. Regardless of much theoretical success in PT-symmetric quantum theory,[33,34] it becomes highly challenging in search of such an elusive Hamiltonian in real physical world. On the other hand, experiments with photonics can be intrinsically non-Hermitian due to the co-existence of gain and loss. Indeed, subsequent works[16,35–47] have undermined their relevance of quantum origin, and readily shown striking PT phase transitions in various optical settings by interleaving balanced gain and loss regions. The associated exceptional spectral properties thereupon translate into unique propagation and scattering behaviors for light, including power oscillations,[36] unidirectional invisibility,[37] coherent perfect laser absorbers,[38] single-mode lasers,[39–41] and supersensitive sensors.[42,43]

Despite there is an ongoing effort on designing optical nonreciprocal devices with PT symmetry,[16,35,47] the demonstrated optical isolation mostly relies on asymmetric transmission across the PT transition threshold (or exceptional point). Such isolation may have difficulty in practical applications. It is therefore intriguing to know whether optical isolation could be realized without changing the system's parameters. Thanks to the directional momentum conservation in SBS, besides it enables to construct an on-chip optical isolator with only one Brillouin cavity, this directionality can break down the reciprocity in PT symmetry where a Brillouin cavity is coupled with a passive resonator. In other words, in this latter case, the features on observing PT symmetry from two directions will automatically behave in an asymmetric and nonreciprocal way. As such, we name this phenomenon "nonreciprocal PT symmetry".

To largely explore SBS-enabled optical nonreciprocity, here in our first experiment, we demonstrate a chip-based nonmagnetic optical isolator in a high-Q silica microtoroid[48] resonator by bulk SBS, in which coherent optically driven acoustic waves can give rise to highly unidirectional photon–phonon interactions. Although SBS[49,50] is deemed as the strongest of all optical nonlinear processes, exciting SBS in a chip-scale device[51,52] is technically challenging because of the stringent requirements on materials and device geometry.[53] In comparison with demonstrated isolators based on interband transition[5–7] which often bear large insertion losses and usually have huge geometry sizes, our isolator shows no insertion loss and have a geometrical scale just above 100 µm. In contrast to other isolators based on cavity-optomechanical schemes[19–26] whose linewidths are typically at 100 KHz level and whose frequency separations between pump and signal are usually small, about tens of MHz, our isolator exhibits a larger bandwidth of 0.57 MHz and 11 GHz separation between the pump and signal waves. These improvements lower the practical difficulty to a great extent in filtering out the pump wave, which is crucial in real applications. More importantly, one of the intriguing features of our isolator is that it can be operated by launching signal waves from both sides simultaneously. In addition to the optical isolator with one microcavity, by harvesting the directional momentum conservation inherent in the SBS process, in our second experiment we further report the observation of nonreciprocal PT symmetry in two coupled microtoroid cavities with balanced gain and loss. Here, the bulk SBS is ex-
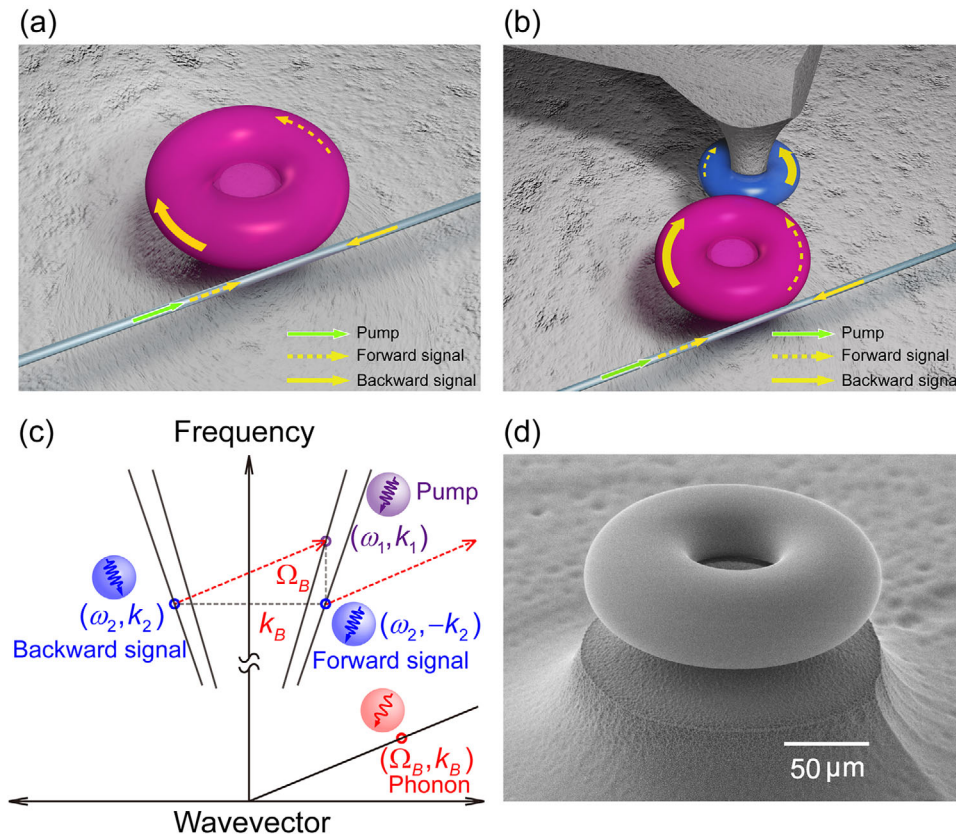
ploited to produce direction-sensitive gain in the Brillouin cavity. In this physical process, the nonreciprocity lifts up the degeneracy of the two exceptional points (EPs) associated with forward and backward transmission (and make the transmissions asymmetric for the frequency in between), which may not only allow to construct an optical isolator but also lead to many other important potential applications.[54,55] As one intriguing application, we theoretically propose to utilize the nonreciprocal PT scheme for the design of a sensitive bi-scale sensor (see Supporting Information, Section S5).

The generation of bulk SBS in a cavity[56–58] requires a phase-matched three-mode system composed of two optical modes and one long-lived propagating acoustic mode in both frequency and momentum space (Supporting Information, Section S1). This process is schematically illustrated in **Figure 1**c, a backward-SBS opto-acoustic interaction is particularly designed to take place within a high-Q microtoroid[48] cavity via properly engineering its geometrical size (Supporting Information, Section S2) (Figure 1a). In experiment (**Figure 2**a), a strong pump laser at frequency ω_p is launched to pump the high-energy optical mode (ω_1, k_1), while a weak tunable signal laser at frequency ω_s is, resonant with a resonator mode, employed to excite the low-energy optical mode (ω_2, k_2) instead. Consequently, the counter-propagating signal mode is expected to undergo strong resonant amplification due to the presence of Brillouin phase matching with the strong pump field and an acoustic wave in the same medium. On the contrary, the co-propagating signal laser remains intact owing to the lack of the available Brillouin scattering. It is this unidirectional Brillouin gain that consents to the realization of a functioning optical isolator as well as nonreciprocal PT symmetric dimer.

2. SBS-Based Optical Isolator

As schematically illustrated in Figure 1a, in our first experiment we perform a series of isolator characterization simply with a Brillouin microresonator at room temperature and atmospheric pressure by simultaneously launching the signal lights from both forward and backward directions through a tapered fiber coupler for optical interface at 1550 nm (the experiment setup is shown in Supporting Information Section S3). Figure 1d is a scanning electron microscope (SEM) image of the fabricated Brillouin microtoroid which has the principle and minor diameters of 175 and 54 µm, respectively. To identify the occurrence of bulk SBS in microtoroid cavity, we first select two high-order optical transverse modes with separation matching the SBS frequency and optically pump the microcavity at the shorter-wavelength mode to above the lasing threshold. As shown in Figure 2b, the Brillouin lasing indeed occurs at the longer-wavelength side. The loaded Q factors for the signal and pump waves are measured to be 1.40×10^8 and 4.36×10^7 with respect to their intrinsic Q factors of 1.99×10^8 and 1.04×10^8, respectively.

To test the isolation performance of the one-cavity device, we start with the case of the same input signal powers from both directions but synchronously changing them, where the signal powers were varied in the range of 1.31–16.44 µW. In this case, the pump light is thermally locked to the shorter-wavelength cavity mode with a blue frequency detuning. During the measure-

**ADVANCED
SCIENCE NEWS**

www.advancedsciencenews.com
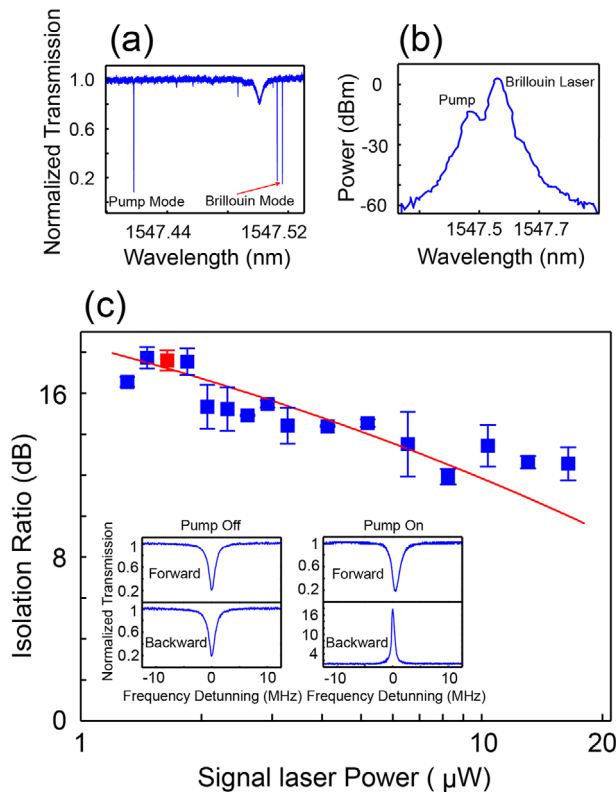
LASER
& PHOTONICS
REVIEWS

www.lpr-journal.org

Figure 1. On-chip optical isolator and nonreciprocal PT symmetry empowered by SBS with whispering-gallery-mode silica microtoroid resonators. a) Schematic illustration of the experiment on optical isolation with a single toroid coupled to a tapered fiber. b) Schematic of the experiment on nonreciprocal PT-symmetry with two toroids coupled with each other and the active one coupled to a tapered fiber. c) Schematic illustration of the requirements on phase and energy conservation conditions for the SBS process. d) SEM image of the Brillouin toroid in our experiments.

ment, the dropped pump power (determined by the power absorbed within the cavity) is kept at 359.82 µW (below the lasing threshold), and the coupling strength κ between the cavity and tapered fiber is fixed at $2\pi \times 0.39$ MHz. As a function of the input signal power, the attained isolation ratio is depicted in Figure 2c where the isolation ratio is defined by the peak power of the backward output signal with respect to the dip signal power in the forward direction. From this point of view, the behavior of our isolator bears essential features of a unidirectional amplifier where the backward power can be further tuned by adding an external optical attenuator if the amplification is undesirable. As one can see, for the launched power range, the isolation ratio is well situated above 11.90 dB and even up to 17.73 dB for the averaged bandwidth of 0.57 MHz. As further indicated in Figure S3 in Supporting Information, in terms of the injected signal power the achievable isolation bandwidth is mainly limited by the linewidth of the cavity mode as well as the Brillouin gain. Despite the narrow isolation bandwidth demonstrated here, it is possible to widen this width by employing a low-Q microcavity or thermally tuning the resonance frequency of the resonator in a broader range. The reduction at higher input powers stems from the Brillouin gain saturation (Supporting Information, Section S6), similar to the reported gain saturation with doped erbium ions.[16] As a comparison, the insets in Figure 2c display typical transmission spectra of the output signals as the pump turned on and off
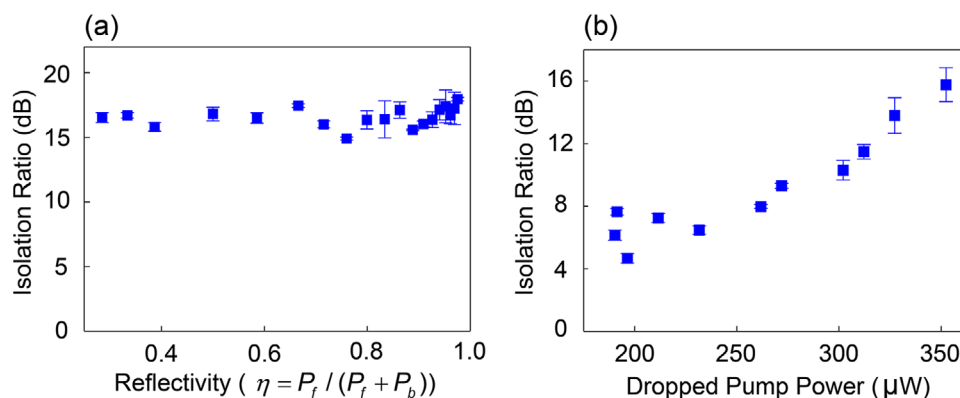
for forward and backward configurations. Without the pump, a Lorentzian dip profile is symmetrically observed in both directions in response to the cavity resonance. In contrast, when turning on the pump, the signal transport is dramatically altered: the forward input still remains the same absorption profile whereas the backward input experiences significant amplification.

Next, we implement the isolation measurements by maintaining the backward input signal power at 3.28 µW while only varying the forward signal power. The dropped pump power and the coupling strength κ are, respectively, set at 359.82 µW and $2\pi \times 0.39$ MHz. Remarkably, as shown in **Figure 3**a, the isolation ratio stays well above 15 dB for the forward input signal power within the range of 1.31–130.56 µW. The observed small fluctuation is mainly due to the instability of the narrow-band tunable optical filter used to filter out the pump light (Supporting Information, Figure S1). To characterize the tunability of our one-cavity isolator, we further conduct an additional assessment in terms of the dropped pump power. In one set of sampling, the recorded experimental data are plotted in Figure 3b with the same signal input powers from both directions at 3.28 µW and the coupling strength of $2\pi \times 0.39$ MHz. As expected, the isolation ratio starts to grow up along with the increase of the dropped pump power from 190.3 to 352.4 µW (below the lasing threshold). Notice that there is no insertion loss for this simple device since the signal light is amplified. Thanks to the fast interaction in SBS, no

ADVANCED
SCIENCE NEWS
www.advancedsciencenews.com

LASER
& PHOTONICS
REVIEWS

www.lpr-journal.org

Figure 2. Optical isolation versus input signal power. a) Transmission spectrum when scanning the laser wavelength across the microtoroid shown in Figure 1d. b) Brillouin lasing spectrum. c) Isolation ratio versus input signal laser power where the equal forward and backward signal laser powers were launched simultaneously from both directions. Inset: Typical transmission spectra corresponding to the red scatter in (c), the red line corresponds to the theoretical curve calculated through the method in (Supporting Information, Section S6).

appreciable signal delay is noticed when the system's parameters are tuned in above measurements. In comparison with other isolation schemes, the SBS-induced optical isolation does reveal some advantages ranging from fast switching, great system stability, large system parameter space, to low input signal power.
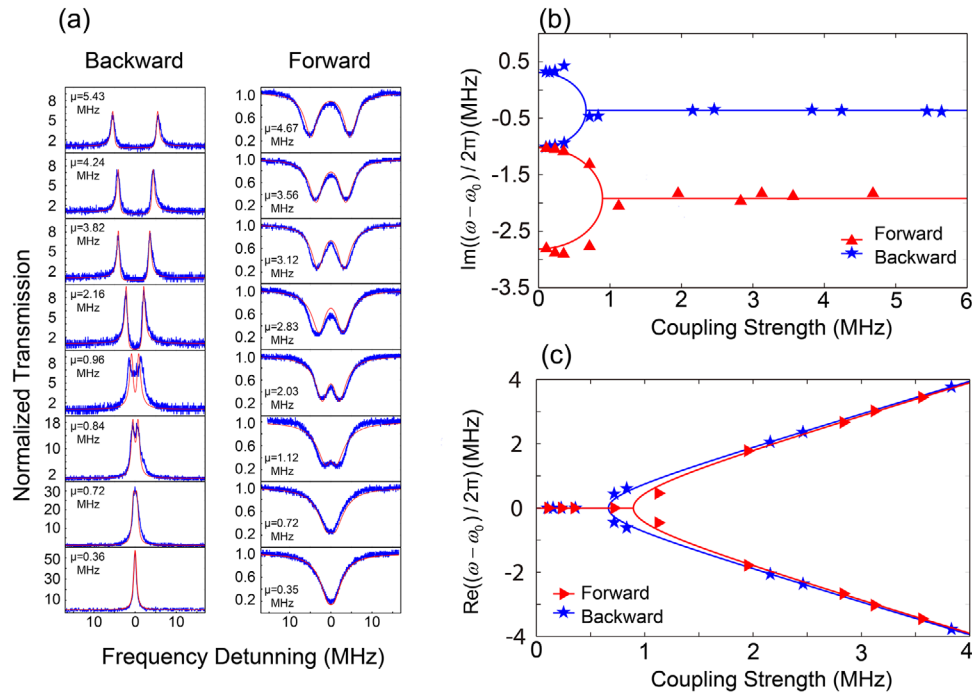
3. SBS-Induced Nonreciprocal PT Symmetry

Thanks to the directional Brillouin gain, the Brillouin microcavity further empowers us to accomplish nonreciprocal PT symmetry by coupling with another passive microtoroid resonator with smaller size. Very recently, we become aware of a theoretical proposal[54] on the realization of nonreciprocal PT phase transition as well as amplification with dynamic gain–loss modulation, which is akin to the physical mechanism we reported in this work. Our second experimental setup is schematically depicted in Figure 1b, where inverted coupling arrangement[59] is adopted. In this part of the experiment, the two microtoroids are mounted on two nanopositioning stages for precise position-separation control. Moreover, we utilize two thermoelectric coolers with a temperature stability of 2 mK to individually tune the cavity resonance wavelength via the thermo-optic effect so that both toroids always share the same resonant frequency during the measurements. The loaded Q factors of the Brillouin cavity are measured to be 3.16×10^7 at 1547.5 nm and 2.96×10^7 at 1547.4 nm, respectively, in contrast to their intrinsic Q-factors at 5.41×10^7 and 9.47×10^7. For the lossy microtoroid, its intrinsic Q factor is 9.72×10^7 at 1547.5 nm.

Since the Brillouin gain is only present in the backward configuration, the PT symmetry is investigated under balanced gain and loss for the backward signal input. While for the forward signal, the system is simply two passively coupled microcavities. To avoid the saturation nonlinearity, the dropped pump power is stabilized at 362.32 μW and the input (backward and forward) signal powers are maintained at a low power of 1.10 μW. In addition, the coupling strength κ between the fiber and Brillouin cavity is fixed at $2\pi \times 2.55$ MHz. After carefully balancing the gain and loss in the backward direction, the evolutions of the transmitted signal spectra are presented in **Figure 4**a by gradually decreasing the coupling strengths $\mu_{f,b}$ between two toroids while maintaining zero cavity frequency detuning. It is apparent that for the backward signal wave, frequency bifurcation induced by PT symmetry exhibits distinct features in spectral location change (Figure 4c) and linewidth narrowing (Figure 4b). In particular, a PT phase transition occurs at the exceptional point where $\mu_b = g = \gamma$. Theoretically, for $\mu_b > \gamma$ the system is in the unbroken phase and two real PT spectral branches $\omega_\pm$ with

Figure 3. Optical isolation performance of the device. a) Measured optical isolation ratio in terms of the reflectivity ($\eta = P_f/(P_f + P_B)$) by setting the backward signal power P_B at 3.28 μW while only varying the power P_f of the forward signal field. The dropped pump power is 359.82 μW and the coupling strength is $2\pi \times 0.39$ MHz. b) Optical isolation as a function of the dropped pump power by fixing both forward and backward signal powers at 3.28 μW. The coupling strength is still $2\pi \times 0.39$ MHz.

**ADVANCED
SCIENCE NEWS**

www.advancedsciencenews.com

LASER
& PHOTONICS
REVIEWS

www.lpr-journal.org

Figure 4. Transmission spectra in nonreciprocal PT symmetry. a). Output transmission spectra for forward and backward signal propagation configurations. μ: coupling strength between two cavities. (blue: experimental data; red: theoretical curves). b,c) The imaginary parts and real parts of the two eigenfrequencies of the two supermodes as a function of the coupling strength for forward (red triangle) and backward (blue star) signal propagation configurations. Parameters: the dropped pump power is 362.32 µW and the coupling strength between the active cavity and the fiber is $2\pi \times 2.55$ MHz (triangles and stars: experimental data; curves: theoretically plotted).

zero linewidth are quadratically displaced at $\pm\sqrt{\mu_b^2 - \gamma^2}$ away from the central cavity resonance frequency ω_0. When $\mu_b < \gamma$, the PT symmetry spontaneously breaks down and the two spectral eigenvalues $\omega_\pm$ now become a complex conjugate pair. These behaviors have been well confirmed by the experimental results shown in Figure 4b,c. Due to the spectral singularity of the complex optical potential, the significant signal amplification in the backward output (Figure 4a) also verifies the theoretical prediction by Mostafazadeh.[34] For the forward signal mode, on the contrary, we anticipate to have least outputs at the two supermodes $\varpi_\pm = -i\frac{\gamma+\gamma_g}{2} \pm \sqrt{\mu_f^2 - (\frac{\gamma-\gamma_g}{2})^2}$ (Supporting Information, Section S4), which are determined by μ_f and the decay rates (γ, γ_g) of the two microresonators. The measured output spectra in Figure 4 show excellent agreements with the above theoretical analysis. As such, nonreciprocal PT symmetry is successfully demonstrated in this compound microcavity system. As shown in Figure 4b,c, the observed EPs associated with two opposite directions are nondegenerate from each other. We notice that in a recent theoretical study,[54] some interesting phenomena have been studied with nonreciprocal PT symmetry. As further illustrated in the Supporting Information, these two nondegenerate EPs behave anisotropically, i.e., when approached from both directions, the sensitivities to the deviations of the two supermodes function differently. This unique behavior provides us with the possibility to realize a bi-scale supersensitive optical sensor which can detect particles of different sizes at the same time (Supporting Information, Section S5). A latest study based on two coupled acoustic cavities has reported a similar behavior.[55] Besides of sensing

applications, the nonreciprocal PT symmetry system could have the potential to build a tunable isolator, akin to the one proposed in ref. [60].

4. Conclusions

Unlike previous demonstrations, the bulk SBS-induced optical nonreciprocity offers many appealing features beyond other alternatives. Despite the demonstrated isolation bandwidth is less than 1 MHz, we believe this width could be extendable by orders of magnitude with further design optimizations including using a microcavity with lower Q-factor or thermally tuning the cavity resonance frequency. From the device integration standpoint, the Brillouin microtoroid resonator has the advantages of compact footprint with CMOS compatibility and reliable isolation functionality, which are crucial in making nonreciprocal elements for on-chip photonic integration. As a fundamental building block, the structure allows a large operating range for the signal power from hundreds of nanowatts to tens of microwatts. Moreover, the scheme could be in principle extendable to squeezed light and continuous variables where phase (in)sensitive parametric amplification is mostly involved in generation. Furthermore, the introduction of nonreciprocal PT symmetry not only affirms the speculation on PT-assisted optical isolation, but also opens up new possibilities for constructing novel PT optical devices outperforming conventional facilities. Although here the SBS is used to demonstrate nonreciprocal PT phase transition, we believe that

other direction-sensitive mechanisms can be also exploited to realize the similar phenomenon.

Supporting Information

Supporting Information is available from the Wiley Online Library or from the author.

Conflict of Interest

The authors declare no conflict of interest.

[1] D. Jalas, A. Petrov, M. Eich, W. Freude, S. Fan, Z. Yu, R. Baets, M. Popović, A. Melloni, J. D. Joannopoulos, M. Vanwolleghem, C. R. Doerr, H. Renner, *Nat. Photonics* **2013**, *7*, 579.

[2] R. J. Potton, *Rep. Prog. Phys.* **2004**, *67*, 717.

[3] L. Bi, J. Hu, P. Jiang, D. H. Kim, G. F. Dionne, L. C. Kimerling, C. A. Ross, *Nat. Photonics* **2011**, *5*, 758.

[4] B. J. H. Stadler, T. Mizumoto, *IEEE Photonics J.* **2014**, *6*, 1.

[5] I. K. Hwang, S. H. Yun, B. Y. Kim, *Opt. Lett.* **1997**, *22*, 507.

[6] Z. Yu, S. Fan, *Nat. Photonics* **2009**, *3*, 91.

[7] L. D. Tzuang, K. Fang, P. Nussenzveig, S. Fan, M. Lipson, *Nat. Photonics* **2014**, *8*, 701.

[8] S. Hua, J. Wen, X. Jiang, Q. Hua, L. Jiang, M. Xiao, *Nat. Commun.* **2016**, *7*, 13657.

[9] K. Wang, Y. Shi, A. S. Solntsev, S. Fan, A. A. Sukhorukov, D. N. Neshev, *Opt. Lett.* **2017**, *42*, 1990.

[10] L. Fan, J. Wang, L. T. Varghese, H. Shen, B. Niu, Y. Xuan, A. M. Weiner, M. Qi, *Science* **2012**, *335*, 447.

[11] M. S. Kang, A. Butsch, P. St. J. Russel, *Nat. Photonics* **2011**, *5*, 549.

[12] M. Krause, H. Renner, E. Brinkmeyer, *Electron. Lett.* **2008**, *44*, 691.

[13] X. Huang, S. Fan, *J. Lightwave Technol.* **2011**, *29*, 2267.

[14] C. G. Poulton, R. Pant, A. Byrnes, S. Fan, M. J. Steel, B. J. Eggleton, *Opt. Express* **2012**, *20*, 21235.

[15] K. Saha, Y. Okawachi, O. Kuzucu, M. Menard, M. Lipson, A. L. Gaeta, in *Conf. Lasers and Electro-Optics*, Optical Society of America, Washington, DC **2013**.

[16] L. Chang, X. Jiang, S. Hua, C. Yang, J. Wen, L. Jiang, G. Li, G. Wang, M. Xiao, *Nat. Photonics* **2014**, *8*, 524.

[17] V. Grigoriev, F. Biancalana, *Opt. Lett.* **2011**, *36*, 2131.

[18] L. D. Bino, J. M. Silver, M. T. M. Woodley, S. L. Stebbings, X. Zhao, P. Del'Haye, *Optica* **2018**, *5*, 279.

[19] Z. Shen, Y. Zhang, Y. Chen, C. Zou, Y. Xiao, X. Zou, F. Sun, G. Guo, C. Dong, *Nat. Photonics* **2016**, *10*, 657.

[20] F. Ruesink, M.-A. Miri, A. Alu, E. Verhagen, *Nat. Commun.* **2016**, *7*, 13662.

[21] K. Fang, J. Luo, A. Metelmann, M. H. Matheny, F. Marquardt, A. A. Clerk, O. Painter, *Nat. Phys.* **2017**, *13*, 465.

[22] Z. Shen, Y.-L. Zhang, Y. Chen, F.-W. Sun, X.-B. Zou, G.-C. Guo, C.-L. Zou, C.-H. Dong, *Nat. Commun.* **2018**, *9*, 1797.

[23] F. Ruesink, J. P. Mathew, M.-A. Miri, A. Alù, E. Verhagen, *Nat. Commun.* **2018**, *9*, 1798.

[24] J. Kim, M. C. Kuzyk, K. Han, H. Wang, G. Bahl, *Nat. Phys.* **2015**, *11*, 275.

[25] J. Kim, S. Kim, G. Bahl, *Sci. Rep.* **2017**, *7*, 1647.

[26] C. Dong, Z. Shen, C. Zou, Y. Zhang, W. Fu, G. Guo, *Nat. Commun.* **2015**, *6*, 6193.

[27] Y. Choi, C. Hahn, J. W. Yoon, S. H. Song, P. Berini, *Nat. Commun.* **2017**, *8*, 14154.

[28] Y. Shi, Z. Yu, S. Fan, *Nat. Photonics* **2015**, *9*, 388.

[29] Y. Zhang, Q. Du, C. Wang, T. Fakhrul, S. Liu, L. Deng, D. Huang, P. Pintus, J. Bowers, C. A. Ross, J. Hu, L. BI, *Optica* **2019**, *6*, 473.

[30] L. Feng, R. El-Ganainy, L. Ge, *Nat. Photonics* **2017**, *11*, 752.

[31] R. El-Ganainy, K. G. Makris, M. Khajavikhan, Z. H. Musslimani, S. Rotter, D. N. Christodoulides, *Nat. Phys.* **2018**, *14*, 11.

[32] C. M. Bender, S. Boettcher, *Phys. Rev. Lett.* **1998**, *80*, 5243.

[33] C. M. Bender, *Rep. Prog. Phys.* **2007**, *70*, 947.

[34] A. Mostafazadeh, *Int. J. Geom. Methods Mod. Phys.* **2010**, *07*, 1191.

[35] B. Peng, Ş. K. Özdemir, F. Lei, F. Monif, M. Gianfreda, G. Long, S. Fan, F. Nori, C. M. Bender, L. Yang, *Nat. Phys.* **2014**, *10*, 394.

[36] C. E. Ruter, K. G. Makris, R. El-Ganainy, D. N. Christodoulides, M. Segev, D. Kip, *Nat. Phys.* **2010**, *6*, 192.

[37] L. Feng, Y. Xu, W. S. Fegadolli, M. Lu, J. E. B. Oliveira, V. R. Almeida, Y. Chen, A. Scherer, *Nat. Mater.* **2013**, *12*, 108.

[38] Z. J. Wong, Y. Xu, J. Kim, K. O'Brien, Y. Wang, L. Feng, X. Zhang, *Nat. Photonics* **2016**, *10*, 796.

[39] L. Feng, Z. J. Wong, R. M. Ma, W. Wang, X. Zhang, *Science* **2014**, *346*, 972.

[40] H. Hodaei, M. A. Miri, M. Heinrich, D. N. Christodoulides, M. Khajavikhan, *Science* **2014**, *346*, 975.

[41] N. Zhang, Z. Gu, K. Wang, M. Li, L. Ge, S. Xiao, Q. Song, *Laser Photonics Rev.* **2017**, *11*, 170052.

[42] W. Chen, S. K. Ozdemir, G. Zhao, J. Wiersig, L. Yang, *Nature* **2017**, *548*, 192.

[43] H. Hodaei, A. U. Hassan, S. Wittek, H. Garcia-Gracia, R. El-Ganainy, D. N. Christodoulides, M. Khajavikhan, *Nature* **2017**, *548*, 187.

[44] A. Regensburger, C. Bersch, M.-A. Miri, G. Onishchukov, D. N. Christodoulides, U. Pesche, *Nature* **2012**, *488*, 167.

[45] Z. Zhang, Y. Zhang, J. Sheng, L. Yang, M.-A. Miri, D. N. Christodoulides, B. He, Y. Zhang, M. Xiao, *Phys. Rev. Lett.* **2016**, *117*, 123601.

[46] P. Peng, W. Cao, C. Shen, W. Qu, J. Wen, L. Jiang, Y. Xiao, *Nat. Phys.* **2016**, *12*, 1139.

[47] J. Wen, X. Jiang, L. Jiang, M. Xiao, *J. Phys. B: At., Mol. Opt. Phys.* **2018**, *51*, 222001.

[48] D. K. Armani, T. J. Kippenberg, S. M. Spillane, K. J. Vahala, *Nature* **2003**, *421*, 925.

[49] R. Y. Chiao, C. H. Townes, B. P. Stoicheff, *Phys. Rev. Lett.* **1964**, *12*, 592.

[50] E. Garmire, *New J. Phys.* **2017**, *19*, 011003.

[51] B. J. Eggleton, C. G. Poulton, P. T. Rakich, M. J. Steel, G. Bahl, *Nat. Photonics 13*, 664, **2019**.

[52] R. Pant, D. Marpaung, I. V. Kabakova, B. Morrison, C. G. Poulton, B. J. Eggleton, *Laser Photonics Rev.* **2014**, *8*, 653.

[53] H. Lee, T. Chen, J. Li, K. Y. Yang, S. Jeon, O. Painter, K. J. Vahala, *Nat. Photonics* **2012**, *6*, 369.

[54] A. Y. Song, Y. Shi, Q. Lin, S. Fan, *Phys. Rev. A* **2019**, *99*, 013824.

[55] K. Ding, G. Ma, Z. Q. Zhang, C. T. Chan, *Phys. Rev. Lett.* **2018**, *121*, 085702.

[56] G. P. Agrawal, in *Nonlinear Fiber Optics*, 5th ed., Academic Press, **2013**, Ch. 9.

[57] M. Tomes, T. Carmon, *Phys. Rev. Lett.* **2009**, *102*, 113601.

[58] Q. Lu, S. Liu, X. Wu, L. Liu, L. Xu, *Opt. Lett.* **2016**, *41*, 1736.

[59] G. Li, X. Jiang, S. Hua, Y. Qin, M. Xiao, *Appl. Phys. Lett.* **2016**, *109*, 261106.

[60] F. Nazari, N. Bender, H. Ramezani, M. K. Moravvej-Farshi, D. N. Christodoulides, T. Kottos, *Opt. Express* **2014**, *22*, 9574.